

by N-WASP (Fig. 4B and fig. S7, C to E). The results suggest that nebulin modules and the N-WASP WH2 domains cooperate to nucleate an unbranched actin filament. Then the actin filament might elongate along the nebulin modules from the Z band toward the center of a sarcomere (fig. S8A).

We assessed the requirement of N-WASP for IGF-1-induced actin filament formation in myofibrils and muscle hypertrophy by RNA interference (RNAi) (fig. S9). EGFP- $\alpha$ -actin coexpressed with control small interfering RNA (siRNA) in the fasted mouse muscle was diffusely distributed without IGF-1 stimulation but located to the Z bands and thin filaments within 2 hours after the stimulation (Fig. 4C and fig. S9D). In contrast, EGFP- $\alpha$ -actin coexpressed with siRNA1 or 2 (fig. S11A) remained diffusely distributed after the stimulation. Therefore, N-WASP is indispensable for the recruitment of  $\alpha$ -actin to the Z bands and for myofibrillar actin filament formation.

IGF-1 administration to mice caused muscle hypertrophy owing to the increase in myofiber volume. The expression of siRNA1 or 2 reduced the cross-sectional area of the myofibers regardless of IGF-1 administration (Fig. 4D and figs. S10 and S11). Thus, N-WASP plays essential roles in both age-dependent natural hypertrophy and administered IGF-1-induced hypertrophy. N-

WASP seems to participate in myofiber hypertrophy by inducing myofibrillar actin filament formation through the nebulin-N-WASP complex. This notion is consistent with the observation that *Neb*-deficient mice develop a muscle atrophy-like phenotype (15, 16).

We elucidated the signaling of IGF-1-induced myofibrillar actin filament formation from the Z bands (fig. S8B) and a mechanism of actin nucleation [supporting online material (SOM) text]. The Neb-N-WASP complex formed by the signaling can explain actin filament formation arising from the Z bands. These findings may provide insights into the mechanisms of muscular diseases, such as nemaline myopathy, caused by *NEB* gene mutations (17). The actin filament formation together with myosin filament assembly, which might also induced by IGF-1 signaling, results in myofibrillogenesis required for muscle maturation and hypertrophy.

#### References and Notes

1. D. J. Glass, *Int. J. Biochem. Cell Biol.* **37**, 1974 (2005).
2. F. Mourkioti, N. Rosenthal, *Trends Immunol.* **26**, 535 (2005).
3. T. Takenawa, S. Suetsugu, *Nat. Rev. Mol. Cell Biol.* **8**, 37 (2007).
4. T. D. Pollard, G. G. Borisy, *Cell* **112**, 453 (2003).
5. M. A. Chesarone, B. L. Goode, *Curr. Opin. Cell Biol.* **21**, 28 (2009).

6. B. Qualmann, M. M. Kessels, *Trends Cell Biol.* **19**, 276 (2009).
7. R. Dominguez, *Crit. Rev. Biochem. Mol. Biol.* **44**, 351 (2009).
8. S. Labeit, B. Kolmerer, *J. Mol. Biol.* **248**, 308 (1995).
9. K. Ojima *et al.*, *J. Cell Biol.* **150**, 553 (2000).
10. A. S. McElhinny, S. T. Kazmierski, S. Labeit, C. C. Gregorio, *Trends Cardiovasc. Med.* **13**, 195 (2003).
11. A. Kontrogianni-Konstantopoulos, M. A. Ackermann, A. L. Bowman, S. V. Yap, R. J. Bloch, *Physiol. Rev.* **89**, 1217 (2009).
12. B. D. Manning, L. C. Cantley, *Cell* **129**, 1261 (2007).
13. E. Paunola, P. K. Mattila, P. Lappalainen, *FEBS Lett.* **513**, 92 (2002).
14. M. Pfuhl, S. J. Winder, M. A. Castiglione Morelli, S. Labeit, A. Pastore, *J. Mol. Biol.* **257**, 367 (1996).
15. C. C. Witt *et al.*, *EMBO J.* **25**, 3843 (2006).
16. M.-L. Bang *et al.*, *J. Cell Biol.* **173**, 905 (2006).
17. D. Sanoudou, A. H. Beggs, *Trends Mol. Med.* **7**, 362 (2001).
18. We thank N. Watanabe and T. Itoh for comments. This work was supported by Grants-in-Aid from the Ministry of Education, Culture, Sports, Science, and Technology of Japan and by the Research Grants (17A-10 and 20B-13) for Nervous and Mental Disorders from the Ministry of Health, Labor, and Welfare of Japan.

#### Supporting Online Material

www.sciencemag.org/cgi/content/full/330/6010/1536/DC1

Materials and Methods

SOM Text

Figs. S1 to S11

References

Movies S1 to S10

14 September 2010; accepted 1 November 2010

10.1126/science.1197767

## Genome Evolution Following Host Jumps in the Irish Potato Famine Pathogen Lineage

Sylvain Raffaele,<sup>1\*</sup> Rhys A. Farrer,<sup>1,\*†</sup> Liliana M. Cano,<sup>1,\*</sup> David J. Studholme,<sup>1,‡</sup> Daniel MacLean,<sup>1</sup> Marco Thines,<sup>1,2,3</sup> Rays H. Y. Jiang,<sup>4</sup> Michael C. Zody,<sup>4</sup> Sridhara G. Kunjeti,<sup>5</sup> Nicole M. Donofrio,<sup>5</sup> Blake C. Meyers,<sup>5</sup> Chad Nusbaum,<sup>4</sup> Sophien Kamoun<sup>1§</sup>

Many plant pathogens, including those in the lineage of the Irish potato famine organism *Phytophthora infestans*, evolve by host jumps followed by specialization. However, how host jumps affect genome evolution remains largely unknown. To determine the patterns of sequence variation in the *P. infestans* lineage, we resequenced six genomes of four sister species. This revealed uneven evolutionary rates across genomes with genes in repeat-rich regions showing higher rates of structural polymorphisms and positive selection. These loci are enriched in genes induced in planta, implicating host adaptation in genome evolution. Unexpectedly, genes involved in epigenetic processes formed another class of rapidly evolving residents of the gene-sparse regions. These results demonstrate that dynamic repeat-rich genome compartments underpin accelerated gene evolution following host jumps in this pathogen lineage.

**P**hytophthora *infestans* is an economically important specialized pathogen that causes the destructive late blight disease on *Solanum* plants, including potato and tomato. In central Mexico, *P. infestans* naturally co-occurs with two extremely closely related species, *Phytophthora ipomoeae* and *Phytophthora mirabilis*, that specifically infect plants as diverse as morning glory (*Ipomoea longipedunculata*) and four-o'clock (*Mirabilis jalapa*), respectively. Elsewhere in North America, a fourth related species, *Phytophthora phaseoli*, is a pathogen of lima beans (*Phaseolus lunatus*). Altogether these four *Phytophthora* spe-

cies form a very tight clade of pathogen species that share ~99.9% identity in their ribosomal DNA internal transcribed spacer regions (1). Phylogenetic inferences clearly indicate that species in this *Phytophthora* clade 1c [nomenclature of (2)] evolved through host jumps followed by adaptive specialization on plants belonging to four different botanical families (2, 3). Adaptation to these host plants most likely involves mutations in the hundreds of disease effector genes that populate gene-poor and repeat-rich regions of the 240-megabase pair genome of *P. infestans* (4). However, comparative genome analyses of specialized sister species

of plant pathogens have not been reported, and the full extent to which host adaptation affects genome evolution remains unknown.

To determine patterns of sequence variation in a phylogenetically defined species cluster of host-specific plant pathogens, we generated Illumina reads for six genomes representing the four clade 1c species. We included the previously sequenced *P. infestans* strain T30-4 (4) to optimize bioinformatic parameters (figs. S1 to S3) (5). To estimate gene copy number variation (CNV) in the five resequenced genomes relative to T30-4, we used average read depth per gene and GC content correction (5) (fig. S4). After GC content correction (6), average read depth provided a good estimate of gene copy number in T30-4 (fig. S5). In the other genomes, we detected 3975 CNV events in coding genes, among which there are 1046 deletion events (Fig. 1).

<sup>1</sup>The Sainsbury Laboratory, Norwich Research Park, Norwich NR4 7UH, UK. <sup>2</sup>Biodiversity and Climate Research Centre BiK-F, Senckenberganlage 25, D-60325 Frankfurt (Main), Germany. <sup>3</sup>Department of Biological Sciences, Institute of Ecology, Evolution and Diversity, Johann Wolfgang Goethe University, Siesmayerstraße 70, D-60323 Frankfurt (Main), Germany. <sup>4</sup>Broad Institute of Massachusetts Institute of Technology and Harvard, Cambridge, MA 02141, USA. <sup>5</sup>University of Delaware, Newark, DE 19716, USA.

\*These authors contributed equally to this work.

†Present address: Imperial College London, London SW7 2AZ, UK.

‡Present address: Biosciences, College of Life and Environmental Sciences, University of Exeter, Exeter EX4 4QD, UK.

§To whom correspondence should be addressed. E-mail: sophien.kamoun@tsl.ac.uk

In total, we identified 746,744 nonredundant coding sequence single-nucleotide polymorphisms (SNPs) in the resequenced strains (Fig. 1). We cal-

culated rates of synonymous (dS) and nonsynonymous (dN) substitutions for every gene (5, 7). Average dS divergence rates relative to *P. infestans*

T30-4 were consistent with previously reported species phylogeny (Fig. 1) (2). We detected a total of 2572 genes (14.2% of the whole genome) with dN/dS ratios >1 indicative of positive selection in the clade 1c strains, with the highest number in *P. mirabilis* (1004 genes) (fig. S6). A high proportion of genes annotated as effector genes show signatures of positive selection (300 out of 796) (fig. S6). This supports previous observations that effector genes are under strong positive selection in oomycetes (8–10).

Haas *et al.* (4) reported that the *P. infestans* genome experienced a repeat-driven expansion relative to distantly related *Phytophthora* spp. and shows an unusual discontinuous distribution of gene density. Disease effector genes localize to expanded, repeat-rich and gene-sparse regions of the genome, in contrast to core ortholog genes, which occupy repeat-poor and gene-dense regions (4). We exploited our sequence data to determine the extent to which genomic regions with distinct architecture evolved at different rates. We used statistical tests (table S1) and random sampling

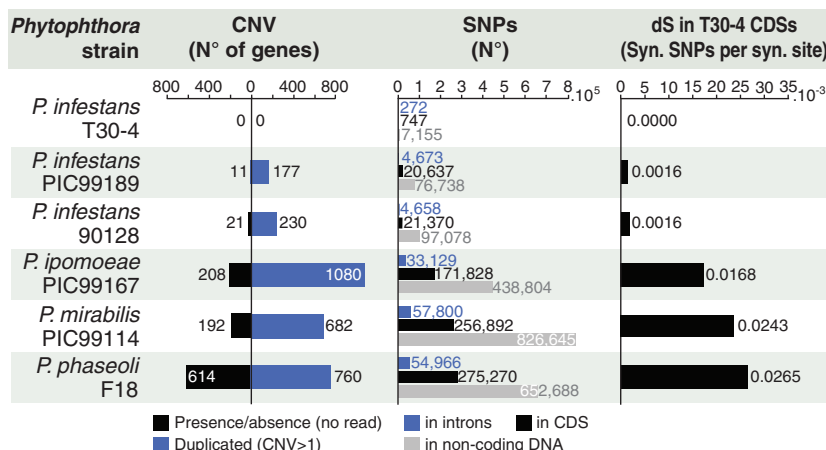


**Fig. 1.** Summary of genome sequences obtained for *Phytophthora* clade 1c species. Six strains representing four species were analyzed. *P. infestans* T30-4 previously sequenced by Haas *et al.* (4) was included for quality control. CDS, coding sequence; CNV, copy number variation; SNP, single-nucleotide polymorphism; syn., synonymous.

**Fig. 2.** The two-speed genome of *P. infestans*. (A) Distribution of copy number variation (CNV), presence/absence (P/A) and single-nucleotide polymorphisms (SNP), and dN/dS in genes from gene-dense regions (GDRs) and gene-sparse regions (GSRs). Statistical significance was assessed by unpaired *t* test assuming unequal variance (CNV, dN/dS); assuming equal variance (SNP frequency); or by Fisher's exact test (P/A) ( $\bullet P < 0.1$ ;  $\bullet\bullet\bullet P < 10^{-4}$ ). Whiskers show first value outside 1.5 times the interquartile range. (B) Distribution of polymorphism in *P. mirabilis* and *P. phaseoli* according to local gene density (measured as length of 5' and 3' flanking intergenic regions, FIRs). The number of genes (P/A polymorphisms) or average values (CNV, SNP, dN/dS) associated with genes in each bin are shown as a color-coded heat map.

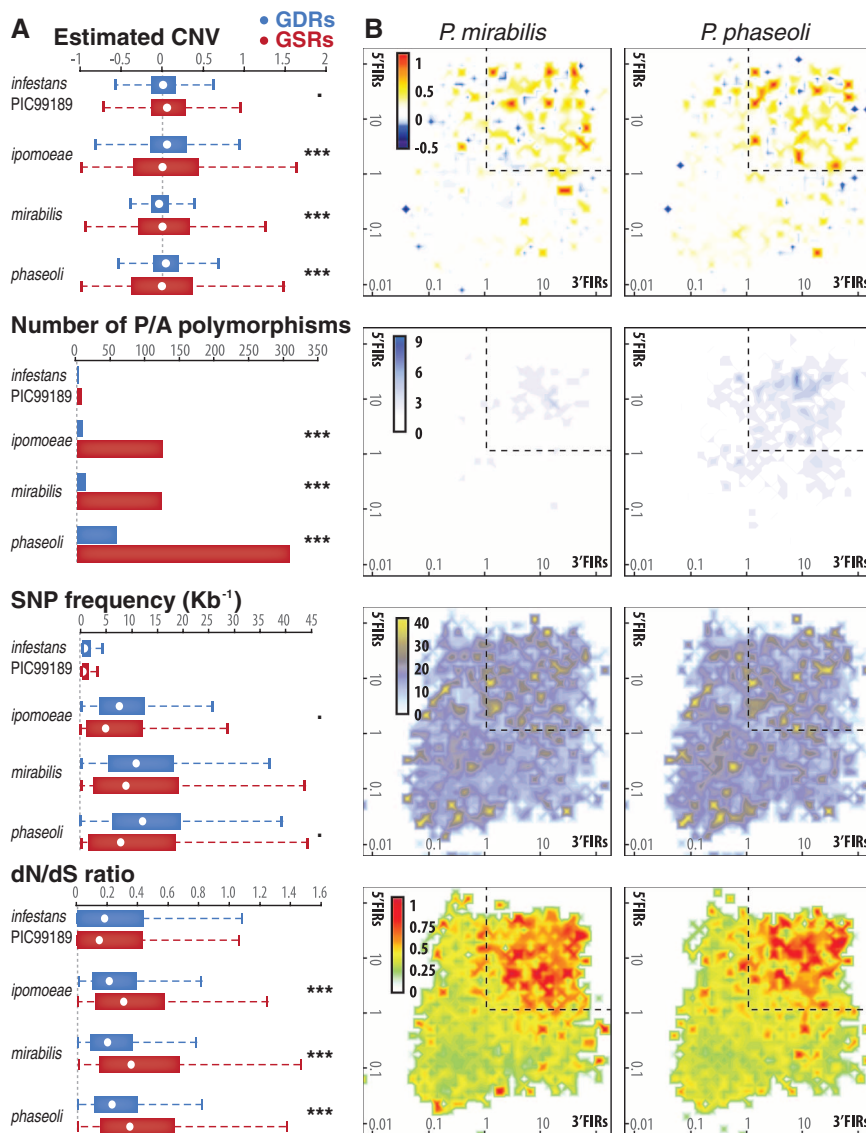


(table S2) to determine the significance of differences in CNV, presence/absence polymorphisms, SNP frequency, and dN/dS values in genes located in gene-dense versus gene-sparse regions (5) (fig. S7 and table S3). Although averages of gene copy numbers were similar in both regions, significantly higher frequency of CNV and gain/loss were observed in genes located in the repeat-rich regions (Fig. 2A and fig. S7). Notably, presence/absence polymorphisms were 13 times as abundant in the gene-sparse compared to the gene-dense regions. In addition, even though SNP frequency was similar across the genomes, average dN/dS was significantly higher in gene-sparse regions, indicating more genes with signatures of positive selection (Fig. 2A). Indeed, 23% of the genes in the gene-sparse regions showed dN/dS > 1 in at least one of the resequenced genomes compared to only 11.5% of genes in the gene-dense regions. In total, 44.6% of the genes in the gene-sparse regions showed signatures of rapid evolution (deletion, duplication, or dN/dS > 1) compared to only 14.7% of the remaining genes. The uneven distribution in gene density in the *P. infestans* genome can be visualized with plots of two-dimensional bins of 5' and 3' flanking intergenic region (FIR) lengths (4). We adapted the plots to illustrate the relationships between gene density and polymorphism and confirmed the increased rates in the gene-sparse regions (Fig. 2B and fig. S8). We conclude that different regions of the examined genomes evolved at markedly different rates, with the gene-sparse, repeat-rich regions experiencing accelerated rates of evolution.

To gain insights into the functional basis of the uneven evolutionary rates detected in the gene-sparse versus gene-dense regions of the clade 1c species, we plotted genome-wide microarray expression data on the FIR length maps (fig. S9) (4). Gene-dense regions were enriched in genes induced in sporangia, the asexual spores that are produced by all *Phytophthora* species. In marked contrast, distribution patterns of genes induced during preinfection and infection stages indicate enrichment in genes located in gene-sparse loci (fig. S9).  $\chi^2$  tests revealed that the relationships between gene density (FIR length) and patterns of gene expression are significant (fig. S9 and table S3). We conclude that the gene-sparse, repeat-rich regions are highly enriched in genes induced in planta, therefore implicating host adaptation in genome evolution.

To assign biological functions to genes with accelerated rates of evolution that populate the gene-sparse, repeat-rich regions, we performed Markov clustering on the predicted proteome of *P. infestans* and implemented gene ontology mapping. Protein families (tribes) significantly enriched or deficient in genes that locate to gene-sparse regions or are rapidly evolving were identified with Fisher's exact test. In total, 811 tribes with five or more proteins were generated (44% of proteome) (figs. S10 and S11). Of these, 163 tribes were statistically enriched in genes from gene-sparse regions (Fig. 3A and fig. S12), 123 tribes

were enriched in fast-evolving genes (fig. S12), and 65 tribes were enriched for both criteria (Fig. 3B and fig. S12). As expected, several of these tribes (19 out of 65) consist of effector families (4, 11–13) (table S4). Other notable tribes include genes encoding various enzymes such as cell wall hydrolases and proteins related to epigenetic maintenance (Fig. 3B and table S4). Surprisingly, tribes annotated as histone and ribosomal RNA (rRNA) methyltransferases were particularly rich in genes located in gene-sparse regions and exhibiting presence/absence polymorphisms (table S4 and figs. S13 and S14). Several genes encoding DOT1-like and SET domain histone methyltransferases and SpoU-like rRNA methyltransferases are exceptional among genes involved in epigenetic maintenance for residing largely in gene-sparse regions and showing high rates of polymorphism (fig. S15).

Our study demonstrates that highly dynamic genome compartments enriched in noncoding sequences underpin accelerated gene evolution following host jumps. Gene-sparse regions that drive the extremely uneven architecture of the *P. infestans* genome are highly enriched in plant-induced genes, particularly effectors, therefore implicating host adaptation as a driving force of genome evolution in this lineage. In addition, we unexpectedly identified several genes involved in epigenetic processes, notably histone methyltransferases, as rapidly evolving residents of the gene-sparse regions. Histone methylation indirectly modulates gene expression in various eukaryotes (14, 15) and could underlie concerted and heritable gene induction patterns through long-range remodeling of chromatin structure (16). Histone acetylation and methylation are thought to be key regulators of gene expression in

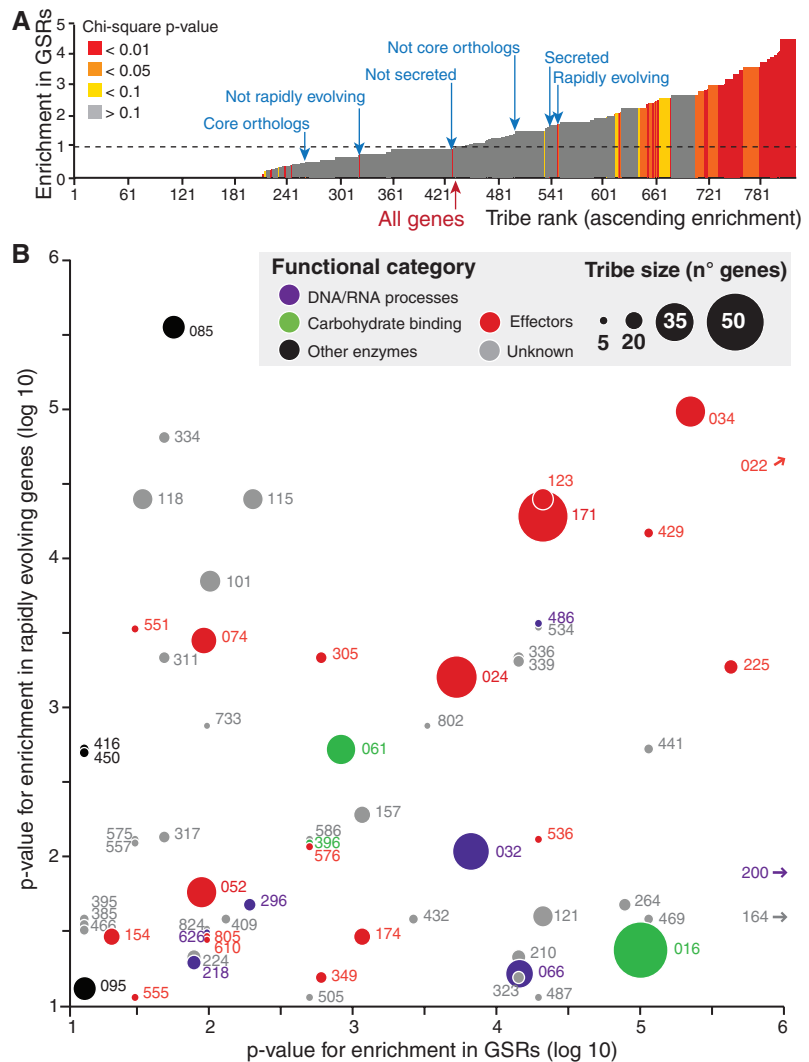


**Fig. 3.** Enrichment of *P. infestans* families (tribes) in genes residing in gene-sparse regions and rapidly evolving genes. **(A)** The 811 *P. infestans* tribes with five or more genes (x axis) ranked on the basis of ascending enrichment in GSR genes (y axis). P value of a  $\chi^2$  test for significance of enrichment is indicated. Additional gene categories (core/not core orthologs, secreted/not secreted, and rapidly/not rapidly evolving) are shown for reference. **(B)** P values of  $\chi^2$  tests for tribe enrichment in GSR genes (x axis) and rapidly evolving genes (y axis). Tribes with P values < 0.1 ( $\log_{10}$ ) are shown. Bubble sizes are proportional to the number of genes in tribes. Bubble colors indicate functional categories. Numbers refer to tribe identifiers as listed in table S4.

*P. infestans* (17) and could modulate expression patterns of genes located in the gene-sparse regions. In addition, histone hypomethylation reduces DNA stability (18, 19) and may have contributed to genome plasticity in the *P. infestans* lineage by regulating transposon activity as well as genomic and expression variability (20, 21). Finally, understanding *P. infestans* genome evolution should prove useful in designing rational strategies for sustainable late blight disease management based on targeting the most evolutionarily stable genes in this lineage.

#### References and Notes

- L. P. Kroon, F. T. Bakker, G. B. van den Bosch, P. J. Bonants, W. G. Flier, *Fungal Genet. Biol.* **41**, 766 (2004).
- J. E. Blair, M. D. Coffey, S. Y. Park, D. M. Geiser, S. Kang, *Fungal Genet. Biol.* **45**, 266 (2008).
- N. J. Grünwald, W. G. Flier, *Annu. Rev. Phytopathol.* **43**, 171 (2005).
- B. J. Haas et al., *Nature* **461**, 393 (2009).
- Materials and methods are available as supporting material on Science Online.
- S. Yoon, Z. Xuan, V. Makarov, K. Ye, J. Sebat, *Genome Res.* **19**, 1586 (2009).
- Z. Yang, R. Nielsen, *Mol. Biol. Evol.* **17**, 32 (2000).
- Z. Liu et al., *Mol. Biol. Evol.* **22**, 659 (2005).
- R. L. Allen et al., *Science* **306**, 1957 (2004).
- J. Win et al., *Plant Cell* **19**, 2349 (2007).
- S. Kamoun, *Annu. Rev. Phytopathol.* **44**, 41 (2006).
- S. K. Oh et al., *Plant Cell* **21**, 2928 (2009).
- M. Tian, E. Huitema, L. Da Cunha, T. Torto-Alalibo, S. Kamoun, *J. Biol. Chem.* **279**, 26370 (2004).
- T. Kouzarides, *Curr. Opin. Genet. Dev.* **12**, 198 (2002).
- Y. Zhang, D. Reinberg, *Genes Dev.* **15**, 2343 (2001).
- L. I. Elizondo, P. Jafar-Nejad, J. M. Clewing, C. F. Boerkoel, *Curr. Genomics* **10**, 64 (2009).
- P. van West et al., *Microbiology* **154**, 1482 (2008).
- A. H. Peters et al., *Cell* **107**, 323 (2001).
- J. C. Peng, G. H. Karpen, R. S. Hawley, *PLoS Genet.* **5**, e1000435 (2009).
- D. W. Zeh, J. A. Zeh, Y. Ishida, *Bioessays* **31**, 715 (2009).
- N. Elango, S. H. Kim, E. Vigoda, S. V. Yi, A. Sidow, *PLOS Comput. Biol.* **4**, e1000015 (2008).

22. We thank the Broad Institute Sequencing Platform and J. Pike for sequencing; G. Kessel and V. Vleeshouwers for biomaterial; and D. Weigel, J. Dangel, and J. Ecker for useful comments. This project was funded by the Gatsby Charitable Foundation, Marie-Curie IEF contract 255104, National Research Initiative of the U.S. Department of Agriculture grant 2006-35600-16623, NSF grant EF-0523670, and research funding program LOEWE of the Ministry of Research, Science and the Arts of Hesse (Germany). Sequences are deposited in GenBank under the submission accession numbers SRA02326–2329 and SRA024355 and in the Short Read Archive under study accession numbers ERP000341–344.

#### Supporting Online Material

www.sciencemag.org/cgi/content/full/330/6010/1540/DC1  
Materials and Methods  
Figs. S1 to S15  
Tables S1 to S4  
References

1 June 2010; accepted 21 October 2010  
10.1126/science.1193070

# Genome Expansion and Gene Loss in Powdery Mildew Fungi Reveal Tradeoffs in Extreme Parasitism

Pietro D. Spanu,<sup>1\*</sup> James C. Abbott,<sup>1†</sup> Joelle Amselem,<sup>2,15†</sup> Timothy A. Burgis,<sup>1†</sup> Darren M. Soanes,<sup>3‡</sup> Kurt Stüber,<sup>4‡</sup> Emiel Ver Loren van Themaat,<sup>4‡</sup> James K. M. Brown,<sup>5‡</sup> Sarah A. Butcher,<sup>1‡</sup> Sarah J. Gurr,<sup>6‡</sup> Marc-Henri Lebrun,<sup>15‡</sup> Christopher J. Ridout,<sup>5‡</sup> Paul Schulze-Lefert,<sup>4‡</sup> Nicholas J. Talbot,<sup>3‡</sup> Nahal Ahmadinejad,<sup>4</sup> Christian Ametz,<sup>1</sup> Geraint R. Barton,<sup>1</sup> Mariam Benjdia,<sup>4</sup> Przemyslaw Bidzinski,<sup>4</sup> Laurence V. Bindschedler,<sup>7</sup> Maike Both,<sup>1</sup> Marin T. Brewer,<sup>8</sup> Lance Cadle-Davidson,<sup>9,10‡</sup> Molly M. Cadle-Davidson,<sup>9</sup> Jerome Collemare,<sup>2§</sup> Rainer Cramer,<sup>7</sup> Omer Frenkel,<sup>8</sup> Dale Godfrey,<sup>11</sup> James Harriman,<sup>9</sup> Claire Hoede,<sup>2</sup> Brian C. King,<sup>8</sup> Sven Klages,<sup>12</sup> Jochen Kleemann,<sup>4</sup> Daniela Knoll,<sup>4</sup> Prasanna S. Koti,<sup>4</sup> Jonathan Kreplak,<sup>2</sup> Francisco J. López-Ruiz,<sup>5</sup> Xunli Lu,<sup>4</sup> Takaki Maekawa,<sup>4</sup> Sirapra Mahanil,<sup>9</sup> Cristina Micali,<sup>4</sup> Michael G. Milgroom,<sup>8</sup> Giovanni Montana,<sup>1</sup> Sandra Noir,<sup>4||</sup> Richard J. O'Connell,<sup>4</sup> Simone Oberhaensli,<sup>13</sup> Francis Parlange,<sup>13</sup> Carsten Pedersen,<sup>11</sup> Hadi Quesneville,<sup>2</sup> Richard Reinhardt,<sup>12</sup> Matthias Rott,<sup>4</sup> Soledad Sacristán,<sup>14</sup> Sarah M. Schmidt,<sup>4¶</sup> Moritz Schön,<sup>4</sup> Pari Skamnioti,<sup>6</sup> Hans Sommer,<sup>4</sup> Amber Stephens,<sup>4</sup> Hiroyuki Takahara,<sup>4</sup> Hans Thordal-Christensen,<sup>11</sup> Marielle Vigouroux,<sup>6</sup> Ralf Weßling,<sup>4</sup> Thomas Wicker,<sup>13</sup> Ralph Panstruga<sup>4\*</sup>

Powdery mildews are phytopathogens whose growth and reproduction are entirely dependent on living plant cells. The molecular basis of this life-style, obligate biotrophy, remains unknown. We present the genome analysis of barley powdery mildew, *Blumeria graminis* f.sp. *hordei* (*Blumeria*), as well as a comparison with the analysis of two powdery mildews pathogenic on dicotyledonous plants. These genomes display massive retrotransposon proliferation, genome-size expansion, and gene losses. The missing genes encode enzymes of primary and secondary metabolism, carbohydrate-active enzymes, and transporters, probably reflecting their redundancy in an exclusively biotrophic life-style. Among the 248 candidate effectors of pathogenesis identified in the *Blumeria* genome, very few (less than 10) define a core set conserved in all three mildews, suggesting that most effectors represent species-specific adaptations.

Filamentous eukaryotes such as fungi and oomycetes (stramenopiles) are responsible for many serious plant diseases. Among these pathogens is a group of taxonomically diverse species, collectively termed obligate biotrophs, which only grow and reproduce on living plants. These microorganisms cause rusts, as well as downy and powdery mildews, and form dedicated invasive infection structures (haustoria) for nutrient uptake. Obligate biotrophs are found in two kingdoms (Stramenopila and Fungi) and in both major fungal phyla (Ascomycota and Basidiomycota), indicating that biotrophy is the result of convergent evolution.

The ascomycete powdery mildews infect ~10,000 angiosperm species, including many important crops (1). They form morphologically complex structures during asexual pathogenesis and produce fruiting bodies (cleistothecia), which develop after sexual reproduction (Fig. 1 and fig. S1).

We sequenced the haploid *Blumeria* genome with the use of Sanger protocols and second-generation methods (table S1) (2). We assembled the sequence reads with a combination of the cortex and CABOG (Celera assembler with the best overlap graph) (3) assemblers into 15,111 contigs ( $L_{50}$ : 18,024 bases;  $L_{50}$  is the length of

the smallest  $N_{50}$  contig, where  $N_{50}$  is the minimum number of contigs required to represent 50% of the genome) on 6898 supercontig scaffolds ( $L_{50}$ : 2,209,085 bases). The overall assembly size is 119,213,040 nucleotides (table S1). We estimate that the actual genome size is ~120 Mb, corresponding to 140-fold coverage of the *Blumeria* genome. We additionally generated draft genome assemblies (~eightfold coverage each) of two other powdery mildew species, *Erysiphe pisi* [pathogenic on pea (*Pisum sativum*)] and *Golovinomyces orontii* (pathogenic on *Arabidopsis thaliana*). Together with *Blumeria*, these species represent three of the five major tribes of the order Erysiphales, which diverged ~70 million years ago (4). We calculated that the genome sizes of the latter two species are ~151 and ~160 Mb, respectively (table

<sup>1</sup>Department of Life Sciences, Imperial College London, London, UK. <sup>2</sup>Institute National de la Recherche Agronomique (INRA), Unite de Recherche Genomique Info, Versailles, France. <sup>3</sup>School of Biosciences, University of Exeter, Exeter, UK. <sup>4</sup>Department of Plant Microbe Interactions, Max-Planck Institute for Plant Breeding Research, Cologne, Germany. <sup>5</sup>Department of Disease and Stress Biology, John Innes Centre, Norwich, UK. <sup>6</sup>Department of Plant Sciences, University of Oxford, Oxford, UK. <sup>7</sup>Department of Chemistry, University of Reading, Reading, UK. <sup>8</sup>Department of Plant Pathology and Plant-Microbe Biology, Cornell University, Ithaca, NY 14853, USA. <sup>9</sup>U.S. Department of Agriculture–Agricultural Research Service Grape Genetics Research Unit, Geneva, NY 14853, USA. <sup>10</sup>Department of Plant Pathology and Plant Microbe Biology, Cornell University, Geneva, NY 14456, USA. <sup>11</sup>Department of Agriculture and Ecology, Faculty of Life Sciences, University of Copenhagen, Copenhagen, Denmark. <sup>12</sup>Max-Planck Institute for Molecular Genetics, Berlin, Germany. <sup>13</sup>Institute of Plant Biology, University of Zürich, Zürich, Switzerland. <sup>14</sup>Centro de Biotecnología y Genómica de Plantas (UPM-INIA) and E.T.S.I. Agrónomos Universidad Politécnica de Madrid, Madrid, Spain. <sup>15</sup>INRA, Unite BIOGER-CPP, Grignon, France.

\*To whom correspondence should be addressed. E-mail: p.spanu@imperial.ac.uk (P.D.S.); panstrug@mpiz-koeln.mpg.de (R.P.)

†These authors contributed equally to this work.

‡These authors contributed equally to this work.

§Present address: Wageningen University, Laboratory of Phytopathology, Wageningen, Netherlands.

||Present address: Institut de Biologie Moléculaire des Plantes–CNRS, Strasbourg, France.

¶Present address: Plant Pathology, Swammerdam Institute for Life Sciences, University of Amsterdam, Amsterdam, Netherlands.